



On induction effects of geomagnetic daily variations from equatorial electrojet and solar quiet sources at low and middle latitudes

Alexei Kuvshinov,^{1,2} Chandrasekharan Manoj,³ Nils Olsen,⁴ and Terence Sabaka⁵

Received 22 January 2007; revised 15 June 2007; accepted 26 July 2007; published 23 October 2007.

[1] We investigate the spatiotemporal behavior of the magnetic vertical component, Z , of the daily ionospheric current systems: the equatorial electrojet (EEJ) and solar quiet (Sq) variations, considering induction in the mantle and oceans. The inducing EEJ and Sq current systems are provided by the comprehensive model of Sabaka et al. (2004). The three-dimensional (3-D) conductivity model of the Earth includes oceans of laterally variable conductance and a spherical conductor (1-D) underneath. Our model studies demonstrate that induction effects in Z due to the EEJ are negligible everywhere inland for all local times. At CHAMP altitude (400 km) the magnetic signal induced by EEJ above the oceans does not exceed 2–5% of the external field during local noon. This, in particular, means that considering the induction effects is not necessary when modeling the EEJ current strength from inland surface magnetic measurements and/or satellite data. As expected, induction in the oceans strongly affects the Sq field. The model studies show that the anomalous induction effect (defined as the difference between results obtained with 1-D and 3-D conductivity models) of Sq is substantial at CHAMP altitude, comprising 50% of the total field. It is therefore necessary to consider induction in the oceans when modeling Sq variations for both ground-based and satellite data. Finally, we demonstrate that the anomalous behavior of the daily variations in Z at south Indian sites, namely, a large positive prenoon peak, can be explained by 3-D induction of the Sq variations, with no contribution from the EEJ.

Citation: Kuvshinov, A., C. Manoj, N. Olsen, and T. Sabaka (2007), On induction effects of geomagnetic daily variations from equatorial electrojet and solar quiet sources at low and middle latitudes, *J. Geophys. Res.*, 112, B10102, doi:10.1029/2007JB004955.

1. Introduction

[2] The equatorial electrojet (EEJ) is an intense eastward flowing current system in the ionospheric E layer at an altitude of about 110 km and aligned with the geomagnetic dip equator on the sunlit side of the Earth. The EEJ has a latitudinal width of 6° – 8° and manifests itself on the ground as more than a threefold increase in the daily variations of the magnetic horizontal component H near the dip equator. The solar quiet (Sq) current system, primarily driven by solar tidal winds, is spread within a latitudinal limit of $\pm 60^{\circ}$ on the sunlit side of the Earth, with an anticlockwise (clockwise) vortex in the Northern (Southern) Hemisphere. Viewed from the Sun, the Earth rotates underneath these

ionospheric current systems, and therefore EEJ and Sq are mainly local time (LT) phenomena. For more information on EEJ, see the reviews by Forbes [1981], Rastogi [1989], and Onwumechili [1997]. The magnetic vertical component Z due to these ionospheric current systems has opposite sign north and south of the dip equator. Besides the primary effect of ionospheric currents, observations of geomagnetic variations are affected by secondary currents induced in the solid Earth and the oceans by the time-varying magnetic field of ionospheric origin.

[3] Electromagnetic induction effects due to the EEJ have been discussed in many publications [cf. Dolginov, 1972; Fambitakoye, 1973; Mayaud, 1973; Van'yan et al., 1975; Ducruix et al., 1977; Yacob, 1977; Samapth and Sastry, 1979; Bhattacharyya, 1981; Carlo et al., 1982; Srivastava and Prasad, 1982; Agarwal and Weaver, 1990; Vassal et al., 1998; Arora and Subba Rao, 2002; Rastogi, 2004] that attempted, in particular, to explain the geomagnetic daily variations in equatorial regions using ground-based, rocket and satellite magnetic measurements, as well as numerical simulations. A topic of special interest is the anomalous daily variation of Z at south Indian (electrojet) stations. From the geometry of the EEJ current system, one expects negative values of Z at locations north of the dip equator, positive values for locations south of the dip equator and

¹Institute of Geophysics, Eidgenössische Technische Hochschule-Zurich, Zurich, Switzerland.

²On leave from Institute of Terrestrial Magnetism, Ionosphere and Radio wave Propagation, Russian Academy of Sciences, Troitsk, Moscow Region, Russia.

³National Geophysical Research Institute, Hyderabad, India.

⁴Danish National Space Center, Copenhagen, Denmark.

⁵Planetary Geodynamics Laboratory, NASA Goddard Space Flight Center, Greenbelt, Maryland, USA.

negligible Z values for locations at the dip equator. In addition, Z should peak around 1200 LT. This behavior of the EEJ was first modelled by *Chapman* [1951] and matches the observations at most equatorial observatories, but not those in south India. The south Indian observatories (located to the north of the dip equator) show a peak around 0900 LT. Moreover, this peak is positive and extends even south of the dip equator [cf. *Rastogi et al.*, 2004]. These quiet day variations in Z cannot be explained by the source field of the EEJ, and there are many hypotheses about the nature of this anomaly (for a review on the subject, see *Rastogi* [2004]). For example, current channelling induced by the EEJ along the Palk Straight (a narrow sea channel between India and Sri Lanka) was invoked by many authors [cf. *Singh et al.*, 1977; *Takeda and Maeda*, 1979; *Papamastorakis and Haerendel*, 1983] to explain the observed anomaly. *Fukushima* [1993] suggested that the anomaly is due to the coastal effects and subsurface conductivity anomalies. Others speculated that the anomaly is an EEJ induction effect from a deep seated conductor beneath south India [cf. *Singh et al.*, 1977; *Rajaram et al.*, 1979; *Thakur et al.*, 1981; *Nityananda and Jayakumar*, 1981]. The diversity of hypotheses indicates that there is no cogent explanation of the south India daily variation anomaly so far. One of the complications is that low-latitude EEJ variations are always superimposed on the Sq field and it is still unclear which source is responsible for the anomalies in the daily variations of geomagnetic fields at equatorial latitudes.

[4] Moreover, while induction by the Sq current system is well understood, induction by the EEJ is still controversial. Simple theoretical estimates [cf. *Schmucker*, 1987] (see also Appendix A) show that for one-dimensional (1-D) models of mantle conductivity, the induced part of daily variations of the EEJ is negligible, due to the small spatial scale of the EEJ (requiring spherical harmonics of $n = 22$ or higher). However, these estimates do not account for large lateral variability in the subsurface conductances due to the distribution of resistive continents and conductive oceans, which substantially influence geomagnetic variations [cf. *Kuvshinov et al.*, 1999, 2002b, 2005; *Olsen and Kuvshinov*, 2004]. In addition, a quantitative estimation of the induction effect requires a spatiotemporal description of the inducing current system. Unlike the Sq current system, which has been modeled by several authors using data from midlatitude geomagnetic observatories [cf. *Schmucker*, 1999], modeling the EEJ is not trivial due to its small spatial scale. It has been common practice to assume a simple source geometry (like an infinite line current) for the EEJ and to account for induction by applying an image current technique [cf. *Jackson*, 1975]. However, it has recently become possible to describe quantitatively the spatiotemporal variations of the EEJ current systems using magnetic measurements from low-orbiting satellites [cf. *Jadhav et al.*, 2002; *Lühr et al.*, 2004; *Sabaka et al.*, 2004; *Le Mouél et al.*, 2006; *Lühr and Maus*, 2006] or by combining ground-based and satellite data [cf. *Manoj et al.*, 2006b].

[5] The first aim of this paper is to perform a comparative study of induction effects computed using realistic models of EEJ and Sq current systems along with a three-dimensional (3-D) conductivity model of the Earth that includes nonuniform oceans of laterally variable conduc-

tance and a spherically symmetric (1-D) conductivity structure underneath.

[6] A second point to be addressed is the simulation of daily variations of Sq and the EEJ (and their induced parts) and comparison with observations. We will investigate whether our 3-D simulations can explain the anomalous daily variations of the vertical magnetic Z component observed at south Indian electrojet stations.

2. Determination of Sq and EEJ Current Systems

[7] Regular daily variations (Sq and EEJ) are mainly generated by horizontal currents in the ionospheric E layer about 110 km above ground. We use the ionospheric current systems predicted by the Comprehensive Model (CM4) of *Sabaka et al.* [2004]. CM4 is based on observatory data and data from the POGO, Magsat, Ørsted and CHAMP satellites, and provides the ionospheric sheet current density $\mathbf{J}_\tau^{\text{ext}}$ at 110 km altitude, as a function of position, local time, season, and solar radio flux $F_{10.7}$. As an example, Figure 1 (left) shows a snapshot of the ionospheric current system at 1230 UT for a reasonably quiet day during spring conditions (21 March 2000). The location of the dip equator is shown in this and the following figures as solid black curves. The main features of Sq (two large current vortices which are symmetric around the dip equator) and the EEJ (current concentration near the dip equator) are clearly visible. There is also a current intensification in auroral regions, reflecting the mean auroral electrojets during quiet conditions. The present version of the Comprehensive Model is not designed to describe these auroral currents in detail, and therefore they will not be considered in the present study. In the following, we will concentrate on low and middle latitudinal current systems during spring equinoctial conditions of the years 1999 and 2000 since data from the key Indian equatorial observatories used in this study are available for these years. Equinoctial days are chosen since the ionospheric current system is most simple (symmetric with respect to dip equator) during these days. The choice of equinoctial days is also motivated by the observation that the anomaly in daily variations of Z at south Indian observatories is most prominent during winter and equinoctial conditions [*Rastogi*, 2004].

[8] For further analysis we have to decouple the Sq and EEJ current systems. We define Sq as the global, large-scale spatial part of the daily variation, and the EEJ as the low-latitude, small-scale spatial part. Specifically, the global Sq current system, $\mathbf{J}_\tau^{\text{ext}, \text{Sq}}(t, \vartheta, \varphi)$ is defined as the low-degree part (up to spherical harmonic degree $n = 15$) of the global ionospheric current system $\mathbf{J}_\tau^{\text{ext}}(t, \vartheta, \varphi)$ as provided by CM4 (which extends to spherical harmonic degree $n = 45$). The residual current system, with spherical harmonic degree, $n > 15$, is attributed to the EEJ currents $\mathbf{J}_\tau^{\text{ext}, \text{EEJ}}(t, \vartheta, \varphi)$. The choice of the limiting spherical harmonic degree, $n = 15$, was a trade-off between the maximum degree required to describe Sq and the minimum degree needed to describe the EEJ. Figure 1 (right) shows a snapshot (for the same day and UT as the left part) of the EEJ current system. Along with the dominant eastward currents of the EEJ, the filtering reveals the return currents to the north and south of the dip equator. This is in good agreement with the morphology of

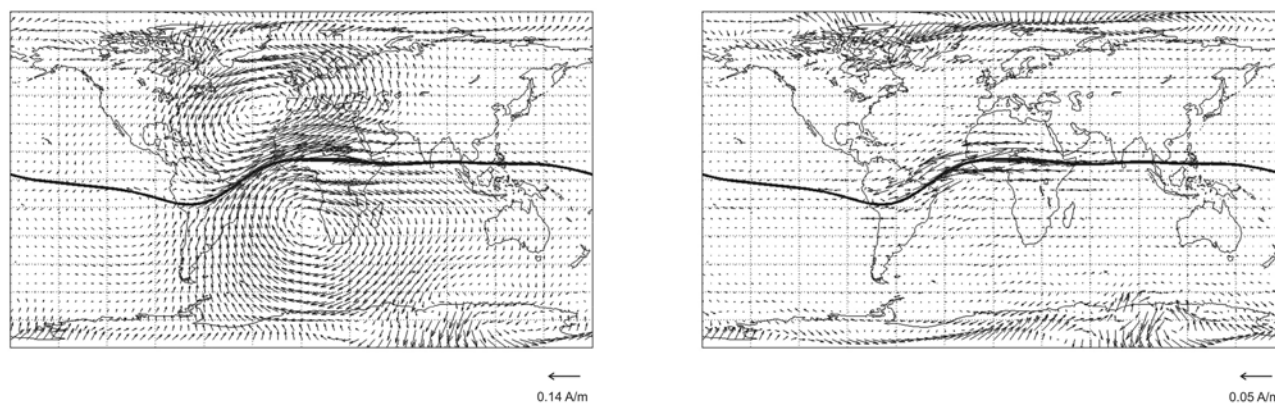


Figure 1. (left) CM4 ionospheric current system (Sq plus EEJ), in A/m. (right) Small-scale part (EEJ) obtained by spatial high-pass filtering of the current system shown in Figure 1 (left). The sheet currents are for 1230 UT on 21 March 2000.

EEJ currents as inferred by *Lühr et al.* [2004] from an analysis of CHAMP magnetic data.

3. The 3-D Conductivity Model of the Earth

[9] Along with the primary (inducing) currents, the electromagnetic (EM) induction simulations require a model of the electrical conductivity of the Earth. Our 3-D model consists of a thin spherical shell of variable conductance $S(\vartheta, \varphi)$ at the Earth's surface and a radially symmetric spherical conductivity $\sigma(r)$ underneath. The shell conductance $S(\vartheta, \varphi)$ is obtained by considering contributions both from seawater and from sediments. The conductance of the sea water has been taken from *Manoj et al.* [2006a] which accounts for ocean bathymetry (taken from the global $5' \times 5'$ NOAA ETOPO map of bathymetry/topography), ocean salinity, temperature and pressure as given by the World Ocean Atlas 2001 (<http://www.ngdc.noaa.gov>). Conductance of the sediments (in continental as well as oceanic regions) is based on the global sediment thicknesses given by the $1^\circ \times 1^\circ$ map of *Laske and Masters* [1997] and calculated by a heuristic procedure similar to that described by *Everett et al.* [2003]. Figure 2 presents the map of the surface shell conductance at $1^\circ \times 1^\circ$ resolution in latitude and longitude. This grid size has been used to solve the induction equations and to calculate the magnetic fields. The underlying spherical symmetric (1-D) conductivity model consists of a 100 km resistive lithosphere of $3000 \Omega m$, and a layered model underneath, which was derived from 5 years of CHAMP, Ørsted, and SAC-C magnetic data by *Kuvshinov and Olsen* [2006].

4. Forward Computation of Induction Due to Sq and EEJ Currents

[10] To simulate daily variations of the electromagnetic (EM) field due to ionosphere currents within a given conductivity models of the Earth, we used the following numerical scheme:

[11] 1. We derive the time harmonics of the primary current system \mathbf{J}_τ^{ext} (either Sq or EEJ) by Fourier transformation. We consider only the first six time harmonics ($p = 1-6$) with periods $24/p$ between 24 and 4 hours; higher time

harmonics are relatively small and conventionally not considered in daily variation analyses [cf. *Schmucker*, 1999].

[12] 2. For each time harmonic, we perform EM induction simulations using 1-D (i.e., without oceans) and 3-D (with oceans) models of electrical conductivity. To simulate magnetic fields, the frequency domain integral equation solution [*Kuvshinov et al.*, 2002a, 2005] is used.

[13] 3. The resulting daily variations are obtained by means of an inverse Fourier transform of the frequency domain results.

5. Global Pattern of Induction Due to Sq and EEJ

[14] We begin with presenting the global maps of the external and induced part of $Z(= -B_z)$, positive downward) calculated at sea level for a fixed local time (LT) of 1230 for all longitudes, on 21 March 2000 (see Figure 3). The induced part, $Z_{ind} = Z_{3D} - Z_{ext}$, is the difference between the total field Z_{3D} (calculated using the 3-D conductivity model with nonuniform oceans) and the external field, Z_{ext} . Results for Sq (large-scale part) are shown in Figure 3 (left); those for the small-scale part (EEJ) are presented in Figure 3

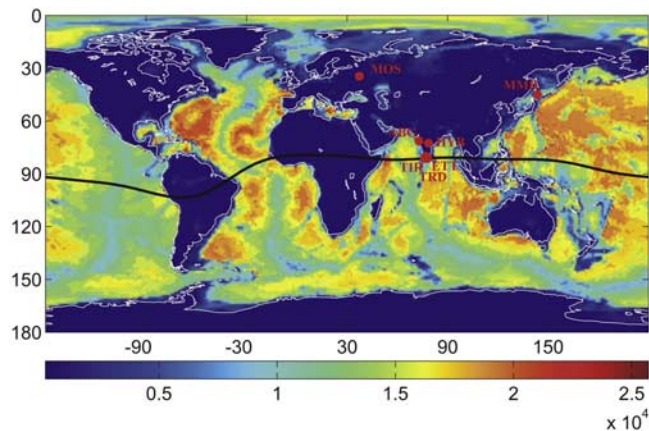


Figure 2. Conductance (in S) of the surface shell describing oceans and sediments. Also shown are the locations of the observatories used in this study.

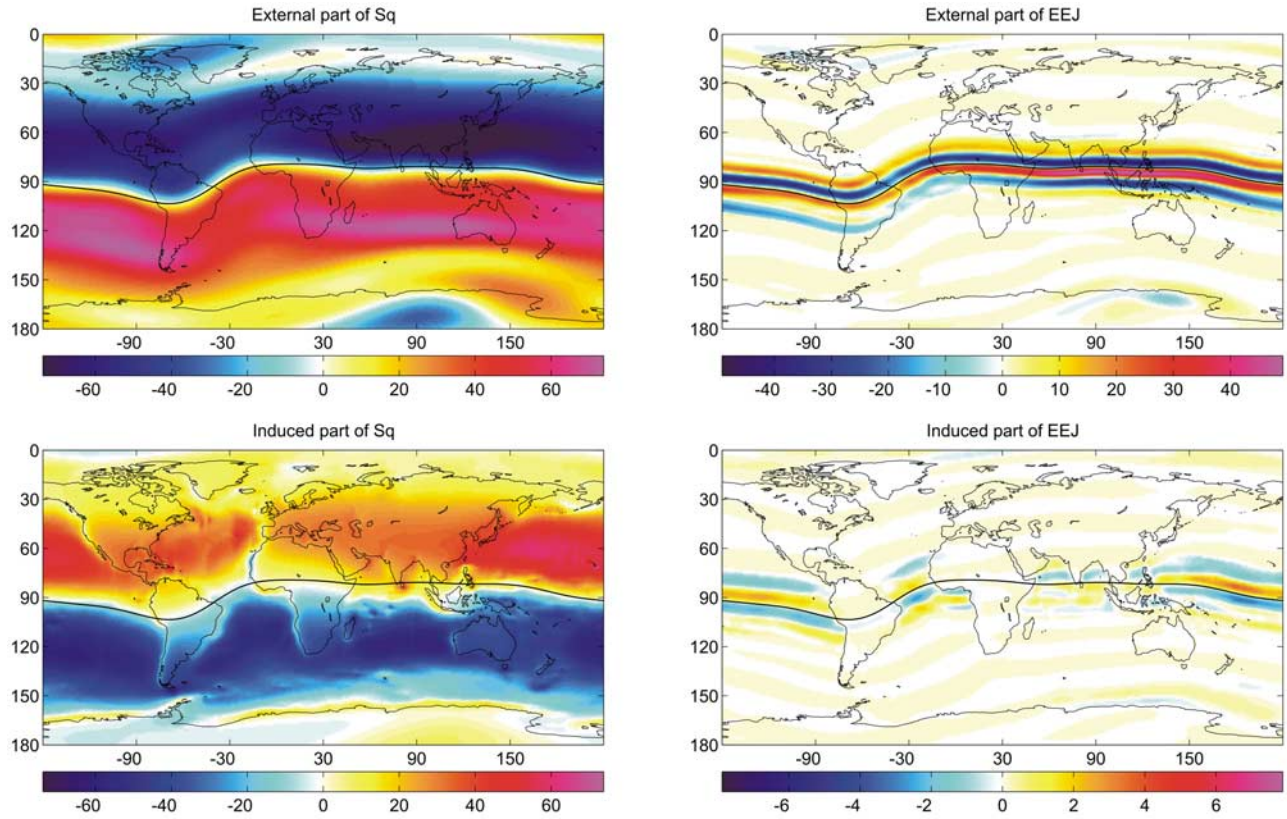


Figure 3. (top) External and (bottom) induced parts of Z (in nT) due to (left) Sq and (right) EEJ at sea level. The results are for 1230 LT of 21 March 2000. Note that different scales are used for external and induced fields of the EEJ (Figure 3, right).

(right). In this section and sections 6 and 7 we mostly discuss the vertical component, as the horizontal components are comparatively less influenced by the induction effects. Note that small-scale auroral contributions are suppressed by smoothly tapering field values poleward of $\pm 19^\circ$ dip latitude to zero when presenting the EEJ results.

[15] The external signals (primary magnetic signals from the ionospheric current systems) reflect the structure of the corresponding ionospheric current systems. For example, Z_{ext} of the EEJ reveals four stripes of alternating signs that follow the dip equator and agree with the geometry of the EEJ currents, a dominant eastward current and weaker return currents to the north and south of the dip equator. The four-stripe structure is most distinctly resolved in the eastern Pacific region for this local time.

[16] As expected, the induced signals in Z at ground have opposite sign compared to the external signal. The induced signal of Sq is of the same order of magnitude as the external signal, reaching 80% of the external in the northern Pacific region. In general, induced signals over continents are smaller than those over oceans both for Sq and EEJ. Moreover, the induced signals of the EEJ are negligible (well below 0.5 nT) inland, including coastal regions. It comprises less than 1% of the maximum external signal (which has an amplitude of about 50 nT at the dip equator for this particular day). The negligible amplitude of the induced signals from the EEJ everywhere inland is in agreement with theoretical estimates (presented in the Appendix) of the induced/external ratio, Q_n , for a 1-D

mantle conductivity model without oceans, due to the small spatial scale of the primary EEJ current system which is described by spherical harmonics of $n \geq \frac{180^\circ}{8^\circ} = 22$ (here 8° is the upper bound on the estimate of the EEJ width). Around local noon (1230 LT), the EEJ induced signal in oceanic regions is small, but not negligible (with maximum amplitude of 3 nT in the eastern Pacific Ocean region, comprising 10% of the external field). Below we will demonstrate that induction during prenoon and afternoon local times is even larger compared to the noon hours, reaching 8 nT over the open seas at 0930 LT. In general, the ratio of predicted induced signals in the oceans to the external signals are in agreement with theoretical estimates of Q_n for the 1-D mantle conductivity model overlaid by a uniform ocean (see Appendix A).

[17] One-dimensional conductivity models, however, do not completely explain the spatiotemporal behavior of Z because the distribution of resistive continents and conductive oceans is nonuniform. Figure 4 presents global maps of the anomalous Z for three LT instants (0930, 1230 and 1530) of the same day. Here we define the anomalous vertical component, Z_{anom} , as the difference between the fields obtained using the 3-D conductivity model and a 1-D model, that is, $Z_{anom} = Z_{3D} - Z_{1D}$. Note that the anomalous field contains only the induced part of the field, since the difference cancels the inducing field which is identical for both the 3-D and 1-D model simulations ($Z_{anom} = Z_{ext} + Z_{ind,3D} - (Z_{ext} + Z_{ind,1D}) = Z_{ind,3D} - Z_{ind,1D}$).

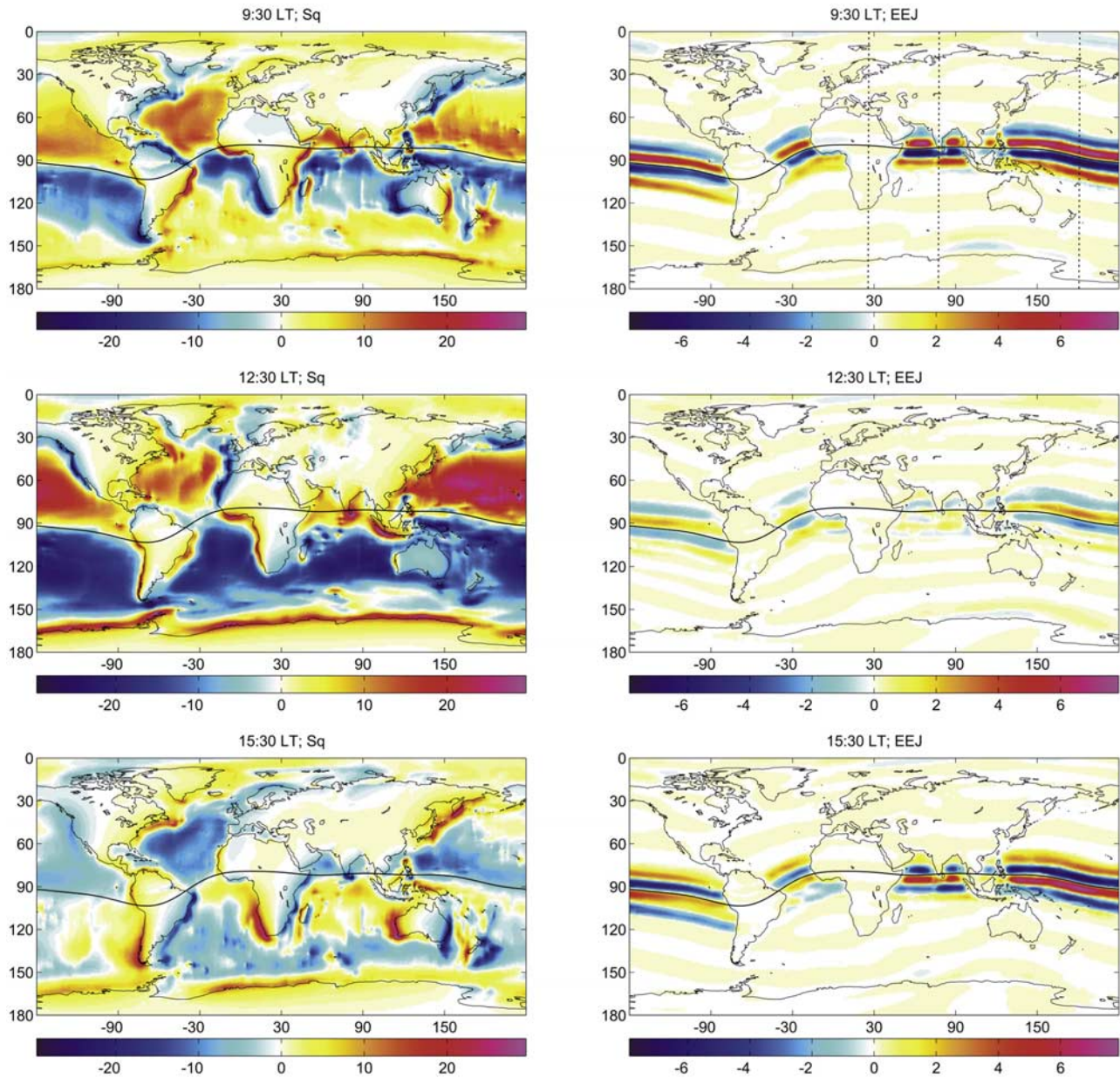


Figure 4. Anomalous Z (in nT) due to (left) Sq and (right) EEJ at sea level for three local time instants on 21 March 2000: (top) 0930 LT, (middle) 1230 LT, and (bottom) 1530 LT.

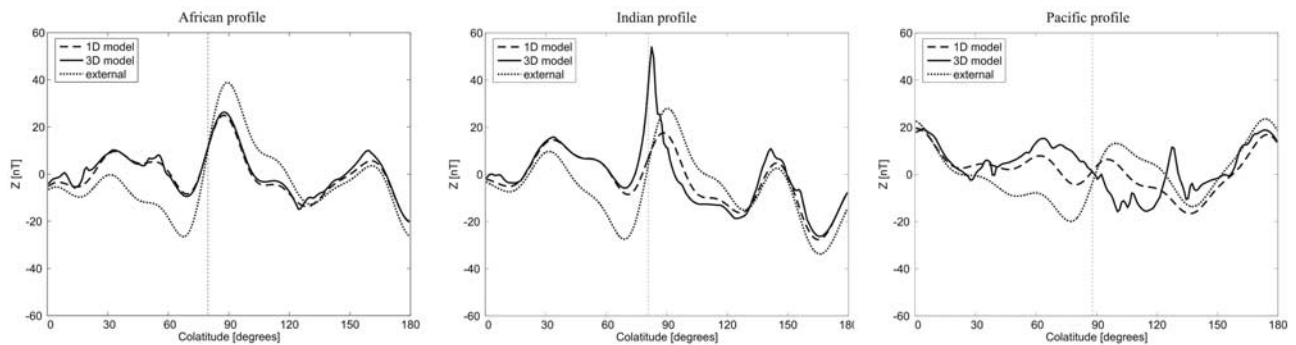


Figure 5. External (dotted) and total (external plus induced) Z obtained using 1-D (dashed) and 3-D (solid) conductivity models, along three longitudinal profiles at sea level. The results are for the large-scale ionospheric currents (Sq) and for 0930 LT on 21 March 2000.

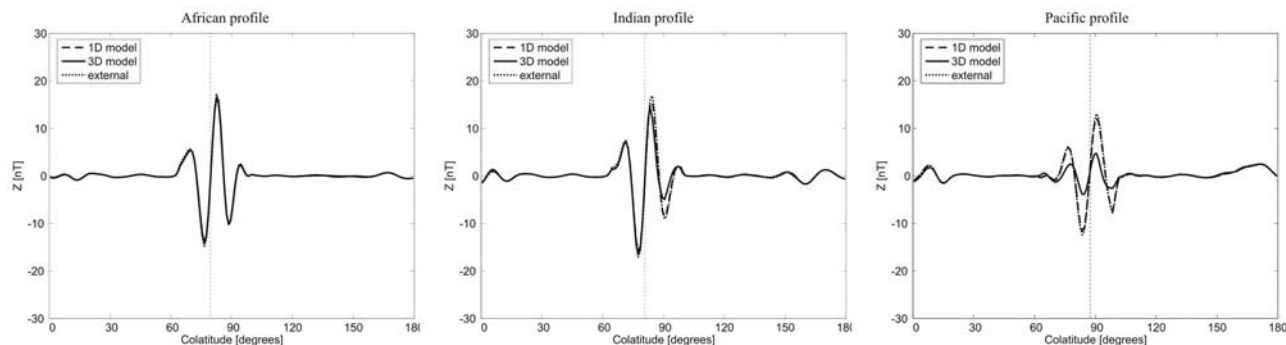


Figure 6. Similar to Figure 5, but for small-scale nonpolar ionospheric currents (EEJ). Note that some profiles are almost identical and therefore not visible.

[18] Results for Sq are presented in Figure 4 (left). As a consequence of the difference between oceanic and continental values, there is an anomalous Z in oceanic regions, with largest amplitudes around noon. However, the most prominent difference between the 3-D and the 1-D results occur in coastal regions. Intensity and sign of these coastal anomalies vary with local time and demonstrate different behavior in different regions of the world. For example, there exist large signals of opposite sign around 0930 and 1530 LT on the western and eastern coasts of Australia, but this anomalous effect is rather small at 1230 LT. Such an anomaly is also observed along the northwestern coast of Africa where the effect is large at local noon but almost absent at 0930 and 1530 LT. Regions with clearly visible anomalous effects near the dip equator include south India and Sri Lanka. Unlike many other coastal regions, this anomaly is present at all investigated local times.

[19] Figure 4 (right) shows results for the EEJ. There are at least three differences compared to Sq: induction from EEJ is (1) confined to oceanic regions; (2) maximum induction signals occur before and after noon; and (3) no coastal anomalies are generated at any of the local times considered.

[20] Figures 5–8 illustrate induction by Sq and EEJ in more detail. Figure 5 shows the external and total (external plus induced) Z component at 0930 LT along three representative profiles. An “African” (28°E) profile is located mainly inland and crosses Europe and Africa from north to south (left to right in the figures). An “Indian” (77°E) profile, which crosses Eurasia and the Indian Ocean, is located approximately half inland and half over the ocean.

Finally, a “Pacific” (180°E) profile is located mainly in the Pacific Ocean. The locations of the profiles are shown as dashed lines in Figure 4 (top right).

[21] From Figures 5 and 7 it is seen that the Sq field shows very different behavior at different longitudes. The vertical dashed lines in Figures 5–8 mark the colatitudes of the dip equator at that longitude. As expected, the 1-D and 3-D results are similar almost everywhere along the “continental” (African) profile (see Figures 5 and 7, right), but differ along the “oceanic” (Pacific) profile (see Figure 5, right, to Figure 8, right). The strongest anomalous behavior is observed along the Indian profile at 0930 LT on the southern coast of India (see Figures 5 and 7, middle), where it reaches 40 nT amplitude. This anomalous peak will be discussed in detail later in the context of the “south Indian anomaly.” As expected, the signals (both for Sq and EEJ) are weaker at 0930 LT compared to 1230 LT. At 0930 LT, the external Sq field in the Pacific region is smaller than the external signals in other profiles. This is probably due to an inaccuracy in the ionospheric currents as provided by the CM4 model for this specific day, as discussed below.

[22] In contrast to Sq, both the 1-D and 3-D results for the Z component of the EEJ, presented in Figures 6 and 8, are very similar and close to the external Z over continental regions as a consequence of the weak induction of the EEJ. However, they differ significantly over the open oceans at 0930 LT. For example, along the Pacific profile the induced signal approaches 8 nT at 0930 LT, comprising 50% of the external signal. Note also that the amplitudes of the side lobes of EEJ as shown in Figures 6 and 8 look somewhat

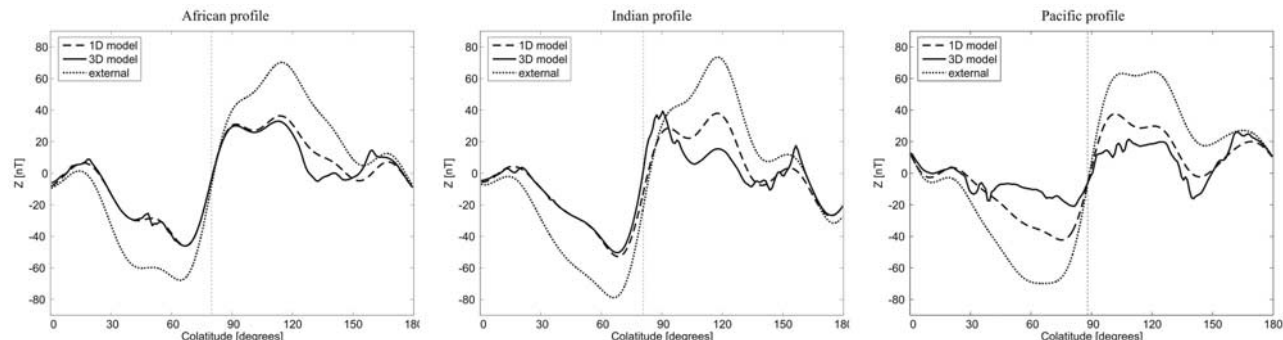


Figure 7. Similar to Figure 5, but for 1230 LT on 21 March 2000.

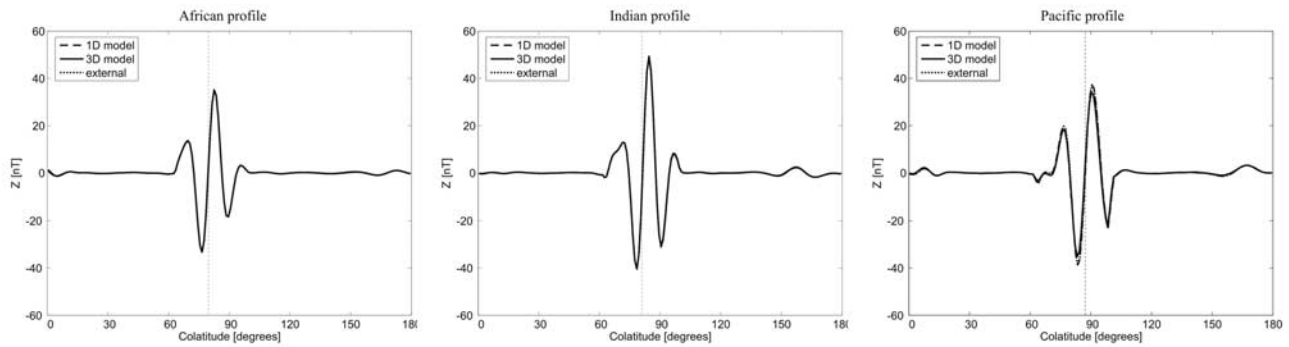


Figure 8. Similar to Figure 6, but for 1230 LT on 21 March 2000.

different from the observations of the vertical component obtained by *Lühr and Maus [2006]*.

[23] It is interesting to estimate the anomalous induction from Sq during local midnight, since satellite data around local midnight are used for determining the core and lithospheric field. It is assumed that nonpolar ionospheric signals are very weak during the night, if not absent. Figure 9 shows the anomalous Z for 2330 LT at sea level and at CHAMP altitude ($h = 400$ km). At sea level the anomalous signals at midnight reach 6–8 nT in many coastal regions (say, in south India and Indonesia) and have a small-scale spatial structure similar to the lithospheric field (and therefore can be erroneously attributed to it). At satellite altitude the anomalous Sq signals are much smoother but still visible, with amplitudes of 2–4 nT. The latter result agrees in general with the estimates of Sq ocean effect at 400 km altitude presented by *Grammatica and Tarits [2002]*.

[24] The model results presented in this paper are based on the ionospheric currents as provided by the CM4 model. However, this model is an approximation of the actual characteristics of the ionospheric currents. In particular CM4 was derived assuming a 1-D electrical conductivity model of the Earth [cf. *Sabaka et al., 2004*]. As a consequence, ocean induction effects are ignored. As CM4 is based not only on observatory data but also on satellite data, this assumption affects the determination of the ionospheric currents, as satellites pass over both continents and oceans. To illustrate the possible amount of distortion, Figure 10 (top) presents global maps of 1-D Z (Figure 10, left) and

anomalous Z (Figure 10, right) due to Sq for 1230 LT at CHAMP altitude ($h = 400$ km). The anomalous (ocean) effect at 400 km altitude is smoother and weaker compared to the ground results (see Figure 4) but still reaches 15 nT in oceanic regions, which amounts to 50% of the total 1-D signal. Thus, assuming a 1-D conductivity model can introduce errors in the determination of ionospheric current systems.

[25] For completeness, Figure 10 (bottom) present analogous results for the EEJ source. One can see that at CHAMP altitude the EEJ induced signal around local noon does not exceed 2–5% of the total signal.

6. Comparison With Observatory Data

[26] We now compare the simulated daily variations with observatory data from south India, where an anomalous behavior of the daily variation of Z has been reported. Figure 11 presents the predicted and observed daily variations as a function of local time on 21 March 2000 at two magnetic observatories near the dip equator, namely, Etaiyapuram (ETT; $\vartheta = 80.83^\circ$, $\varphi = 78.02^\circ$) and Tirunelveli (TIR; $\vartheta = 81.33^\circ$, $\varphi = 77.82^\circ$), the locations of which are shown in Figure 2.

[27] Figure 11 clearly demonstrates the anomalous behavior of the daily variation of Z , namely the large positive prenoon (0930 LT) peak at south Indian observatories close to the dip equator. We subtracted a “true” baseline (rather than the value around midnight) from the absolute daily

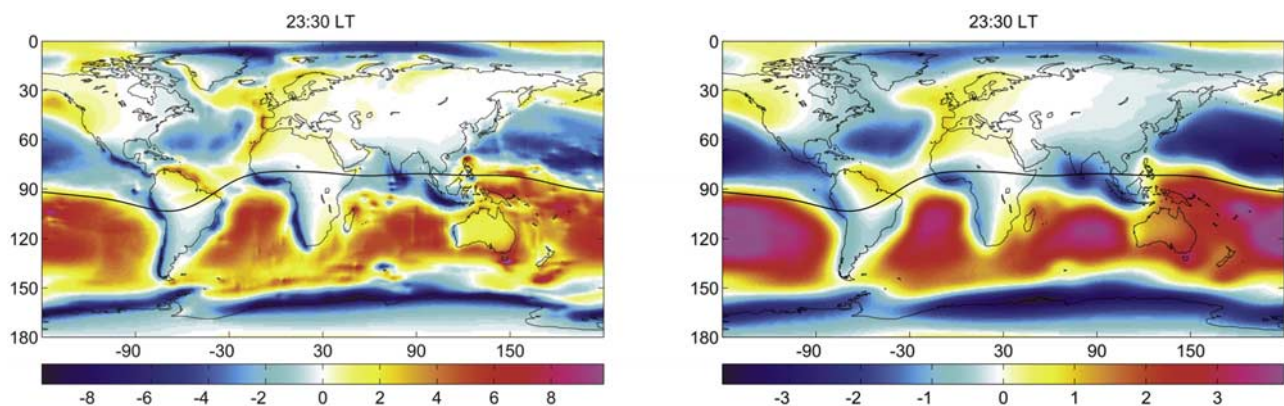


Figure 9. Anomalous Z (in nT) due to Sq at 2330 LT on 21 March 2000 at (left) sea level and (right) CHAMP altitude of 400 km.

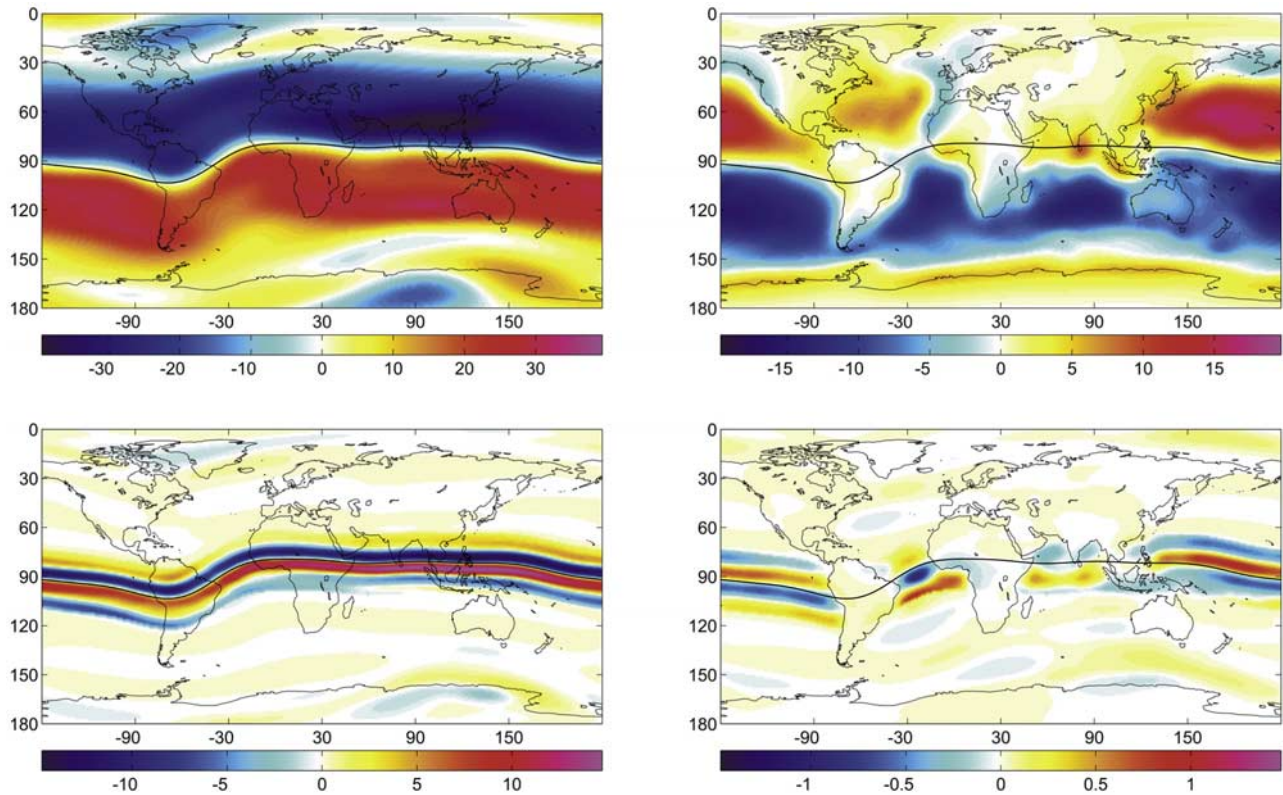


Figure 10. (left) Z (in nT) predicted by a 1-D model, and (right) anomalous Z , due to (top) Sq and (bottom) EEJ for 1230 LT on 21 March 2000 and altitude of 400 km.

variation measured at the observatories. The “true” baseline is defined as the difference between the observed daily mean and that of the external field contribution, as argued by *Schmucker* [1999]. The last results of section 5 also discourage the use of the midnight level as a baseline, especially for south India observatories. The simulated daily variations from 1-D and 3-D model are the sum of the external and induced signals from the respective models. There is a remarkable agreement between the observations

and the 3-D predictions, both regarding peak-to-peak magnitude and the shape of the signals. These results show that the anomalous variations in Z can be completely attributed to 3-D induction.

[28] We further investigate whether the anomalous behavior of Z in south India is due to induction by the large-scale (Sq) or by the small-scale (EEJ) source. Figures 12 (left) and 12 (right) show predicted results for Sq and the EEJ for the observatory TIR. As expected, induction by the

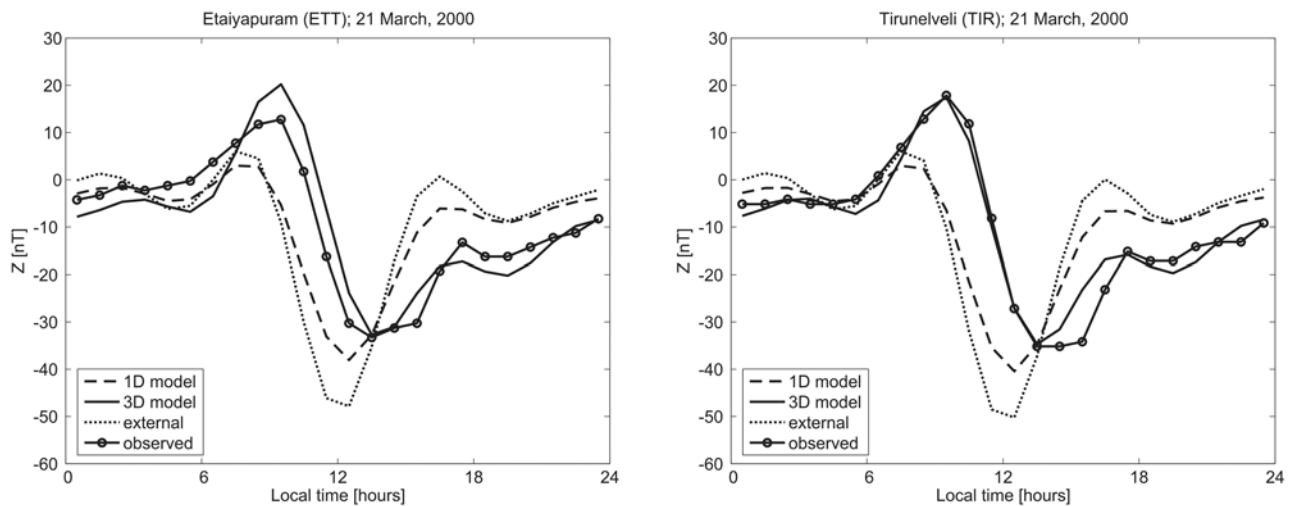


Figure 11. Observed (solid with circles) and predicted daily variations of Z (in nT) as a function of local time on 21 March 2000 for the south Indian observatories (left) Etaiyapuram and (right) Tirunelveli.

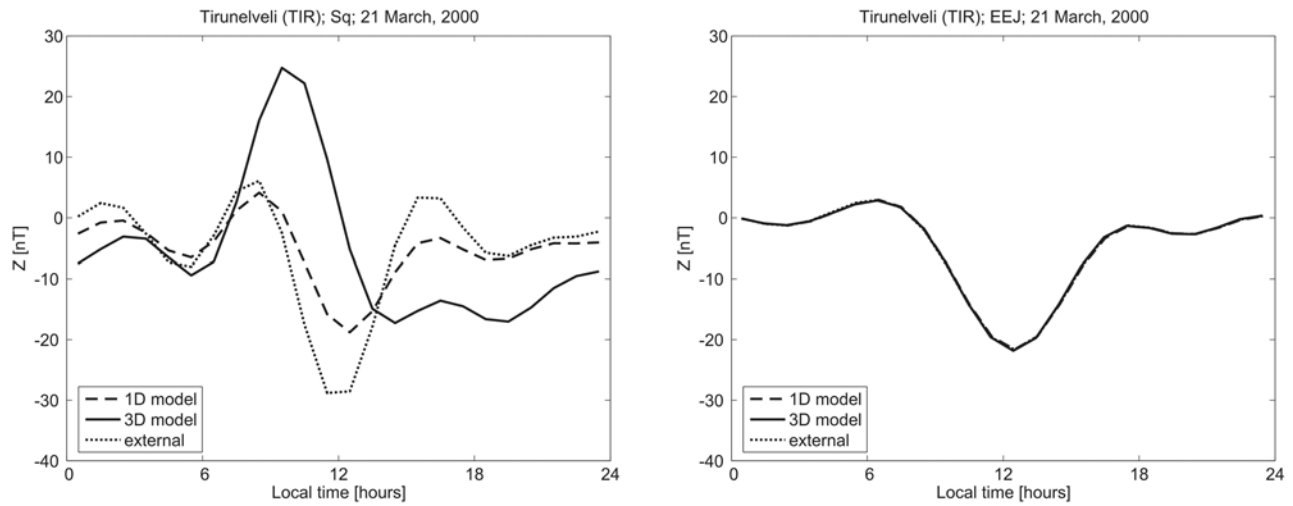


Figure 12. Predicted daily variations of Z due to (left) Sq and (right) EEJ on 21 March 2000 for the south Indian observatory Tirunelveli. Note that some profiles in Figure 12 (right) are almost identical and therefore not visible.

EEJ is negligible at the electrojet sites in India, and the anomalous behavior of Z is fully accounted for by 3-D induction of the large-scale Sq variations. The positive anomaly at 0930 LT also extends south of the dip equator and peaks (latitudinally) over Sri Lanka (as can be seen in Figures 4 and 5). This is well in line with the observations at a site in Sri Lanka as reported by *Rastogi et al.* [2004].

[29] Figure 13 presents a comparison of the daily variation of Z at the two midlatitude observatories Moscow (MOS; $\vartheta = 34.53^\circ$, $\varphi = 37.32^\circ$) and Memambetsu (MMB; $\vartheta = 43.9^\circ$, $\varphi = 144.2^\circ$). The Russian observatory Moscow is located far inland and hence there is no anomalous induction. However, the Japanese observatory Memambetsu, located on the coast near a deep ocean trench, is strongly affected by the ocean effect. However, in contrast to the south Indian sites, the ocean effect at MMB shows up in a different way, namely as a two hour shift of the local noontime peak toward morning hours. Our 3-D predictions

agree very well with the observations, whereas a 1-D model is not able to explain this behavior.

[30] Figure 14 shows predicted and observed daily variations for another equinoctial day (22 March 1999) at the south Indian sites TIR and Trivandrum (TRD; $\vartheta = 81.5^\circ$, $\varphi = 77^\circ$). The anomalous behavior of Z , and the good agreement between the observations and the 3-D predictions are evident. For this day the peak-to-peak amplitudes of the predicted variations (at all investigated sites) are smaller than the observed ones. A possible explanation could be that CM4 is not designed to describe the day-to-day variability of ionosphere currents, since monthly means of $F_{10.7}$ have been used when deriving the model. Since the ratio of the amplitudes of the observed and predicted variations is similar at all the observatories considered on this day, we decided to scale the CM4 predictions by an empirically determined factor which appeared to be twice the $F_{10.7}$ value for this specific day.

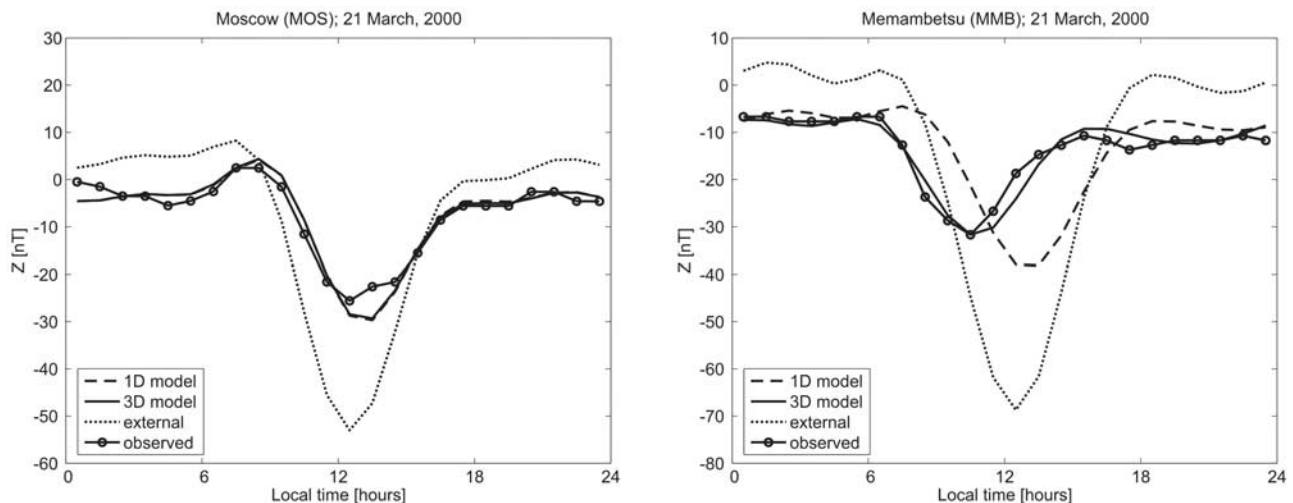


Figure 13. Observed (solid with circles) and predicted daily variations of Z on 21 March 2000 for the Russian observatory (left) Moscow and (right) the Japanese observatory Memambetsu.

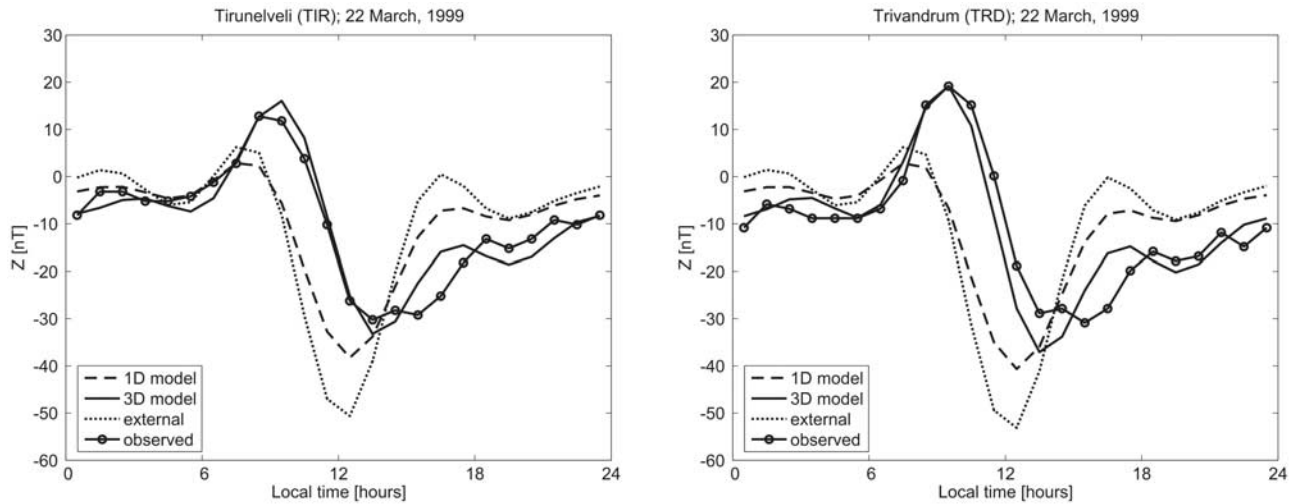


Figure 14. Observed (solid with circles) and predicted daily variations of Z on 22 March 1999 for (left) Tirunelveli and (right) Trivandrum.

[31] Figure 15 shows the predicted and observed daily variations of Z on the same day at the two Indian sites Alibag (ABG; $\vartheta = 71.37$, $\varphi = 72.87$) and Hyderabad (HYB; $\vartheta = 72.58$, $\varphi = 78.55$), located far north of the electrojet. Here the 3-D and 1-D predictions are rather similar (especially at ABG) and show maximum amplitude around noon.

[32] It is also interesting to compare the predicted and observed horizontal component, H , in the Indian sector. Figure 16 shows daily variations of H on 22 March 1999 at the two sites TIR and TRD, where an anomalous behavior of Z is observed. As expected, there is no big difference between the 3-D and 1-D results, since H component is much less influenced by the ocean effect compared to Z . Both observed and predicted H are maximal at 1130 LT. One can also see that the predictions agree rather well with observations, even if they appear to be slightly larger than those observed.

[33] We conclude this section by discussing another anomalous feature of daily variations in the Indian sector.

By analyzing data from closely spaced observatories operated during the International Equatorial Electrojet Year campaign, *Arora et al.* [1993] found that the line of reversing sign in local noon Z (line of zero Z) is more than 150 km north of the dip equator. This is in contrast to the line of peak of H , which aligns with the dip equator (it was expected that these two lines have to coincide). Such a deviation was considered to be one of the most significant feature of the electrojet behavior in the Indian sector. We argue that the shift of zero Z is due to induction in the oceans associated with the large-scale Sq source. Figure 17 supports this argument. It presents total (external plus induced) Z and H components predicted by a 3-D model at 1130 LT on 22 March 1999 along a portion of the Indian profile (77°E). Figure 17 (left) shows the results due to EEJ source. The dashed lines show the locations where Z reverses sign and where H has maximum value. As expected these lines are closely spaced. Figure 17 (right) shows the Z and H components due to unseparated (EEJ

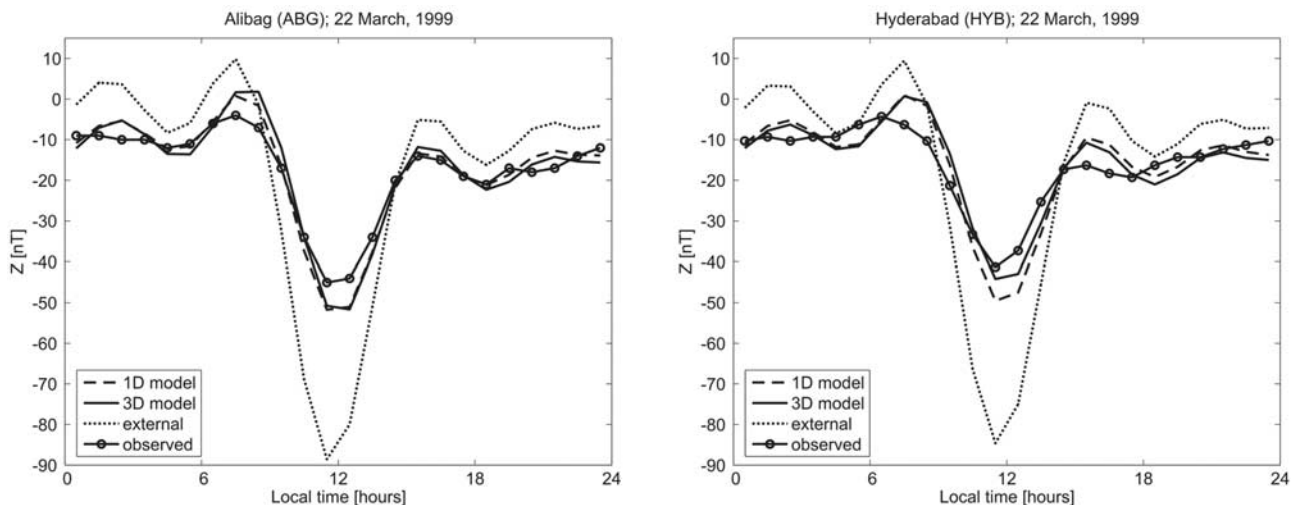


Figure 15. Observed (solid with circles) and predicted daily variations of Z on 22 March 1999 for (left) Alibag and (right) Hyderabad.

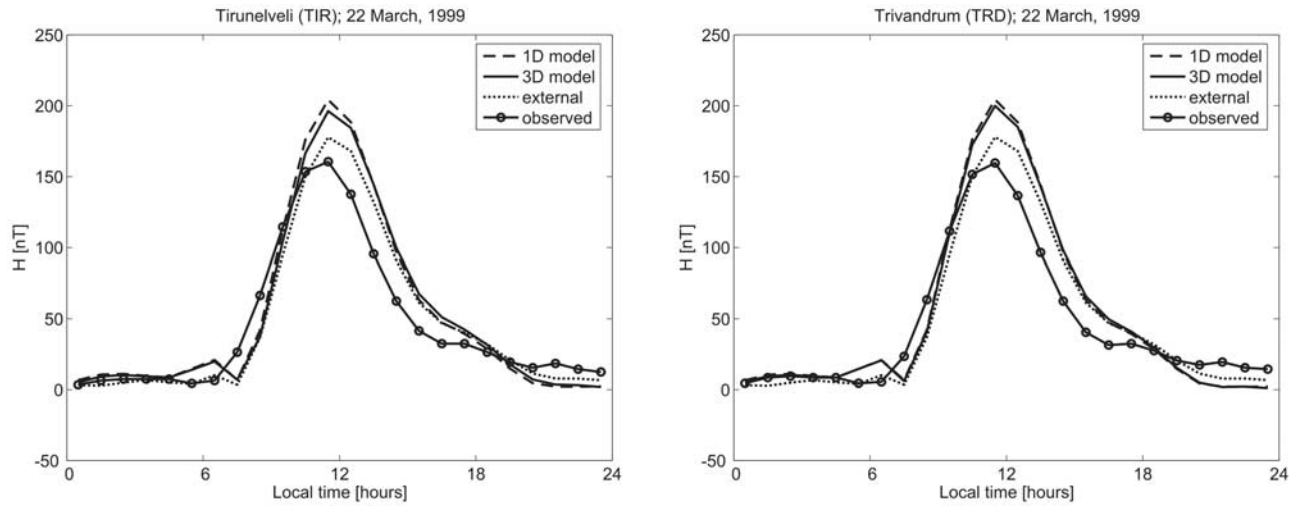


Figure 16. Observed (solid with circles) and predicted daily variations of H on 22 March 1999 for (left) Tirunelveli and (right) Trivandrum.

plus S_q) source. With S_q induction included, the distance between two lines widens to about 170 km. This is consistent with experimentally observed separation. Note, however, that this result has to be taken with caution, since the size of our grid ($1^\circ \times 1^\circ$; this corresponds to a grid spacing of about 110 km at equatorial latitudes) is comparable with the investigated shift. Calculations on more detailed grid are needed to investigate whether this shift is really due to 3-D induction of S_q .

7. Conclusions

[34] We examine the spatiotemporal behavior of the vertical magnetic field of the daily ionospheric current systems (EEJ and S_q), when considering induction in the mantle and oceans.

[35] Our model studies demonstrate that the induction effect in Z due to the EEJ is negligible (comprising 1% of

the external signal) everywhere inland for all local times. Contrary to S_q , no coastal anomalous induction is generated by the EEJ. However, in the open ocean (e.g., in the eastern part of Pacific Ocean) the EEJ induction effect is present, especially at prenoon and afternoon hours, when it can reach 50% of the external signal. Around local noon the induced signal in the ocean amounts to about 10% of the external signal. At CHAMP altitude the EEJ induced signal above the oceans comprises only 2–5% of the external field at local noon. In particular, this means that one need not include induction effects when modeling the EEJ current strength from inland magnetic measurements (including coastal regions) and/or satellite magnetic observations at local noon. Estimation of the EEJ current strength from satellite and ground magnetic data is important in understanding ionospheric processes like vertical plasma uplift, ionospheric conductivity structure, etc. Investigations are ongoing into the nature of the day time EEJ and evening

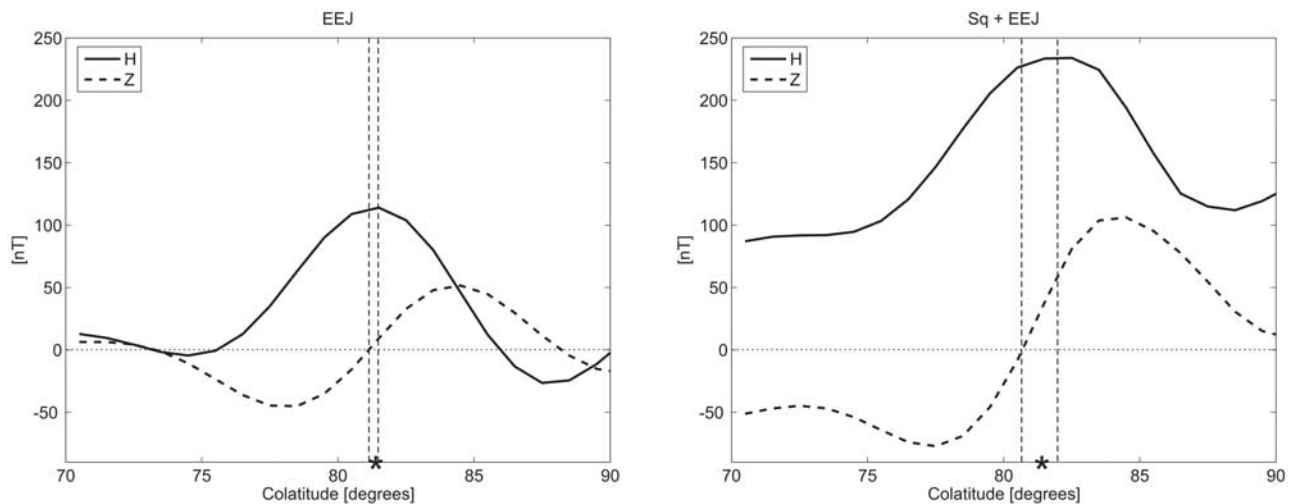


Figure 17. Predicted H (solid) and Z (dashed) at 1130 LT along a portion of the Indian profile ($77^\circ E$) on 22 March 1999. The asterisk on x axis marks the colatitude of the dip equator at this longitude; the vertical dashed lines mark colatitudes where Z reverses sign and where H has maximum value.

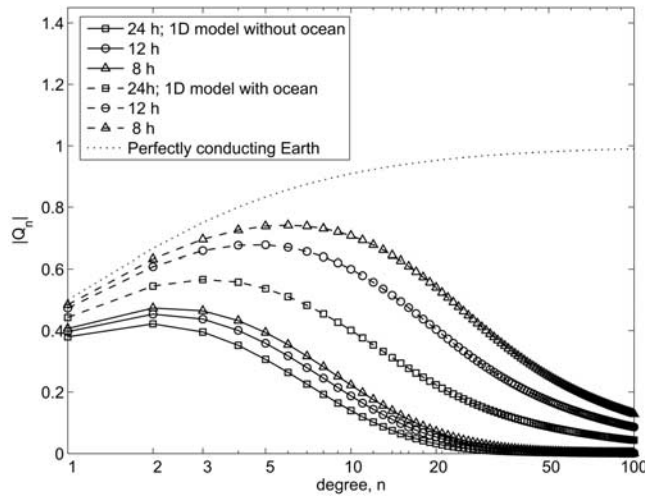


Figure A1. $|Q_n|$ for three time harmonics of daily variations as a function of degree n . Solid lines, $|Q_n|$ for the 1-D mantle conductivity model without oceans. Dashed lines, $|Q_n|$ for the 1-D model with uniform ocean of 15000 S. For comparison, the dotted line shows an upper limit, $n/(n + 1)$, for $|Q_n|$ which corresponds to a perfectly conducting Earth.

ionospheric instabilities. With the upcoming Swarm mission the interest in studying the EEJ using satellite magnetic data is expected to increase. Hence establishing the fact that induction effects of the EEJ are negligible is highly relevant.

[36] As expected, induction in the oceans strongly affects the Sq field in coastal regions. The intensity and the sign of the Sq coastal anomalies vary with local time and show different behavior in different regions of the world. South India and Sri Lanka appear to be regions where prominent coastal anomalies are present during various local times.

[37] The model studies also show that the anomalous induction effect (defined as the difference between results obtained with and without induction in the oceans) of Sq is substantial at CHAMP and Swarm altitudes; Around 1230 LT it reaches 15 nT in oceanic regions (comprising more than 50% of the total field). This means that the ocean effect in Sq variations should be considered in geomagnetic modeling, both regarding ground-based and satellite data.

[38] It is interesting to note that induction in the oceans by Sq generates small-scale anomalies of 8–10 nT intensity at ground even around local midnight in many coastal regions of the world (e.g., in Indonesia, south India, southwest Africa). At CHAMP altitude these anomalies have amplitudes of 2–3 nT. These results are relevant for lithospheric field determination where it is common practice to assume negligible nonpolar ionospheric currents during nighttime.

[39] The most striking find is that the well-known anomalous behavior of the daily variations of Z at Indian electrojet sites, namely a large positive prenoon peak, is entirely attributable to the ocean effect of Sq variations, with the EEJ playing no part. This result also implies that there is no need to assume a deep conductor in this region, which has been suggested to explain the observed anomaly in daily variations of Z . It is remarkable that for all sites considered, our 3-D predictions are in a very good agreement with the observations.

[40] Finally, we show that the ocean effect of Sq is most likely to be responsible for the observed anomalous separation of the line of zero Z from the line of peak H .

[41] The results reported here consider induction due to ionospheric currents at middle and low latitudes, with emphasis on the analysis of Indian observatory data. Work is ongoing to analyze equatorial magnetic signals in other regions of the world.

[42] Movies visualizing the daily variations of EEJ and Sq sources and their associated induced parts on global grids, in both local and universal times and at both sea level and satellite altitude, are available at <http://www.epm.geophys.ethz.ch/~kuvshinov/Sq-EEJ>.

Appendix A: $|Q_n|$ for Time Harmonics of Daily Variations as a Function of Degree n

[43] Outside the conducting Earth, and assuming a laterally uniform conductivity in the Earth, the Fourier components of the magnetic field, $\mathbf{B}(\omega) = -\text{grad } V(\omega)$, can be derived from a scalar magnetic potential V which is approximated by a spherical harmonic expansion

$$V(r, \vartheta, \varphi, \omega) = a \sum_{n=1}^N \sum_{m=-n}^n \left[\epsilon_n^m(\omega) \left(\frac{r}{a}\right)^n + \iota_n^m(\omega) \left(\frac{a}{r}\right)^{n+1} \right] P_n^m \cos \vartheta e^{im\varphi}, \quad (\text{A1})$$

where ϵ_n^m and ι_n^m are the complex expansion coefficients of the external (inducing) and internal (induced) parts of the potential at frequency ω , (r, ϑ, φ) are spherical coordinates, $a = 6371.2$ km is the mean radius of the Earth, ϑ and φ are geographic colatitude and longitude; $P_n^m(\cos \vartheta)$ are the associated Legendre functions. The amount of induction is defined by the ratio of external (inducing) to internal (induced) expansion coefficients, $Q_n(\omega) = \epsilon_n^m(\omega)/\iota_n^m(\omega)$, where Q_n does not depend on order m for any 1-D conductivity structure. Figure A1 presents $|Q_n|$ as a function of degree n for three time harmonics ($24/p$, $p = 1, \dots, 3$) of daily variations. Solid lines show $|Q_n|$ for a continental 1-D conductivity structure (taken from *Kuvshinov and Olsen [2006]*) without oceans. As expected the longer the period of the inducing field, the smaller $|Q_n|$. For large values of n , $|Q_n|$ decreases with increasing n . For example, at a period of 24 h it drops from 0.42 for $n = 2$ (degree of fundamental spherical harmonic of Sq at this period) down to less than 0.05 for $n = 22$ (minimum degree which describes the EEJ). Adding a uniform ocean of 15000 S conductance to the considered model of mantle conductivity substantially changes $|Q_n|$ (compare the dashed lines in Figure A1). $|Q_n|$ becomes larger (stronger induction) when the conductive ocean is added; for example, at a period of 24 h, and for $n = 2$, $|Q_n|$ increases to 0.53. There is a shift of the maxima of $|Q_n|$ to higher n . Although there is a comparable amount of decrease with increasing n , $|Q_n|$ remains significant (with a value of 0.23) for $n = 22$. Note that the dotted line on Figure A1 shows an upper limit, $n/(n + 1)$, for $|Q_n|$ which corresponds to a perfectly conducting Earth.

[44] **Acknowledgments.** We appreciate the respective institutes/organizations for operating the geomagnetic observatories used in the present study. Comments made by Nandini Nagarajan improved an earlier version of this paper. We thank the reviewers Baldev Arora and Hermann

Lühr for their helpful comments. This work is supported in part by the Russian Foundation for Basic Research under grant 06-05-64329-a.

References

- Agarwal, A. K., and J. T. Weaver (1990), A theoretical study of induction by electrojet over a coastline for Sq and substorm periods, *Phys. Earth Planet. Inter.*, *61*, 165–181.
- Arora, B. R., and P. B. V. Subba Rao (2002), Integrated modeling of EM response functions from Peninsular India and Bay of Bengal, *Earth, Planets Space*, *54*, 637–654.
- Arora, B. R., M. V. Mahashabde, and R. Karla (1993), Indian IEEY geomagnetic observational program and some preliminary results, *Braz. J. Geophys.*, *11*, 365–386.
- Bhattacharyya, A. (1981), Induced magnetic field of the equatorial electrojet at the surface of the Earth, *Geophys. J. R. Astron. Soc.*, *67*, 557–563.
- Carlo, L., B. P. Singh, R. G. Rastogi, and A. K. Agarwal (1982), The induced effects of geomagnetic variations in the equatorial region, *J. Geophys.*, *51*, 199–205.
- Chapman, S. (1951), The equatorial electrojet as detected from the abnormal electric current distribution above Huancayo and elsewhere, *Arch. Meteorol. Geophys. Bioklimatol. Sect. A*, *4*, 368–390.
- Dolginov, S. S. (1972), Equatorial electrojet, according to KOSMOS-321 measurements, *Geomagn. Aeron.*, *12*, 611–617.
- Ducruix, J., V. Courtillot, and J. LeMouél (1977), On the induction effects associated with the equatorial electrojet, *J. Geophys. Res.*, *82*, 335–351.
- Everett, M., S. Constable, and C. Constable (2003), Effects of near-surface conductance on global satellite induction responses, *Geophys. J. Int.*, *153*, 277–286.
- Fambitakoye, O. (1973), On the induction effects associated with the equatorial electrojet, *Ann. Geophys.*, *29*, 149–167.
- Forbes, J. (1981), The equatorial electrojet, *Rev. Geophys.*, *19*, 469–504.
- Fukushima, N. (1993), Trans-equatorial field aligned currents at low latitude and their possible connection with the equatorial electrojet, Brazil, *J. Geophys.*, *11*, 291–301.
- Grammatica, N., and P. Tarits (2002), Contribution at satellite altitude of electromagnetically induced anomalies arising from a three-dimensional heterogeneously conducting Earth, using Sq as an inducing source field, *Geophys. J. Int.*, *151*, 913–923.
- Jackson, J. D. (1975), *Classical Electrodynamics*, John Wiley, New York.
- Jadhav, G., M. Rajaram, and R. Rajaram (2002), A detailed study of equatorial electrojet phenomenon using Ørsted satellite observations, *J. Geophys. Res.*, *107*(A8), 1175, doi:10.1029/2001JA000183.
- Kuvshinov, A., and N. Olsen (2006), A global model of mantle conductivity derived from 5 years of CHAMP, Ørsted, and SAC-C magnetic data, *Geophys. Res. Lett.*, *33*, L18301, doi:10.1029/2006GL027083.
- Kuvshinov, A., D. Avdeev, and O. Pankratov (1999), Global induction by Sq and Dst sources in the presence of oceans: Bimodal solutions for non-uniform spherical surface shells above radially symmetric Earth models in comparison to observations, *Geophys. J. Int.*, *137*, 630–650.
- Kuvshinov, A. V., D. B. Avdeev, O. V. Pankratov, S. A. Golyshev, and N. Olsen (2002a), Modelling electromagnetic fields in 3D spherical Earth using fast integral equation approach, in *3D Electromagnetics*, edited by M. S. Zhdanov and P. E. Wannamaker, chap. 3, pp. 43–54, Elsevier, New York.
- Kuvshinov, A. V., N. Olsen, D. B. Avdeev, and O. V. Pankratov (2002b), Electromagnetic induction in the oceans and the anomalous behaviour of coastal C-responses for periods up to 20 days, *Geophys. Res. Lett.*, *29*(12), 1595, doi:10.1029/2001GL014409.
- Kuvshinov, A. V., H. Utada, D. Avdeev, and T. Koyama (2005), 3-D modelling and analysis of DstC-responses in the North Pacific Ocean region, revisited, *Geophys. J. Int.*, *160*, 505–526, doi:10.1111/j.1365-246X.2005.02477.x.
- Laske, G., and G. Masters (1997), A global digital map of sediment thickness, *Eos Trans. AGU*, *78*(46), Fall Meet. Suppl., F483.
- Le Mouél, J.-L., P. Shebalin, and A. Chulliat (2006), The field of the equatorial electrojet from CHAMP data, *Ann. Geophys.*, *24*, 515–527.
- Lühr, H., and S. Maus (2006), Direct observation of the F region dynamo currents and the spatial structure of the EEJ by CHAMP, *Geophys. Res. Lett.*, *33*, L24102, doi:10.1029/2006GL028374.
- Lühr, H., S. Maus, and M. Rother (2004), Noon-time equatorial electrojet: Its spatial features as determined by the CHAMP satellite, *J. Geophys. Res.*, *109*, A01306, doi:10.1029/2002JA009656.
- Manoj, C., A. Kuvshinov, S. Maus, and H. Lühr (2006a), Ocean circulation generated magnetic signals, *Earth, Planets Space*, *58*, 429–439.
- Manoj, C., H. Lühr, S. Maus, and N. Nagarajan (2006b), Evidence for short spatial correlation lengths of the noontime equatorial electrojet inferred from a comparison of satellite and ground magnetic data, *J. Geophys. Res.*, *111*, A11312, doi:10.1029/2006JA011855.
- Mayaud, P. (1973), About the effects induced by the daily variation due to the equatorial electrojet, *J. Atmos. Terr. Phys.*, *36*, 1367–1376.
- Nityananda, N., and D. Jayakumar (1981), Proposed relation between anomalous geomagnetic variations and the tectonic history of south India, *Phys. Earth Planet. Inter.*, *27*, 223–228.
- Olsen, N., and A. Kuvshinov (2004), Modelling the ocean effect of geomagnetic storms, *Earth Planets Space*, *56*, 525–530.
- Onwumechili, C. A. (1997), *The Equatorial Electrojet*, Gordon and Breach, Amsterdam, Netherlands.
- Papamastorakis, I., and G. Haerendel (1983), An analog model of the geomagnetic induction in the south Indian Ocean, *J. Geophys.*, *52*, 61–68.
- Rajaram, U., B. P. Singh, and A. K. Agarwal (1979), Effect of the preserve of a conducting channel between India and Sri Lanka on the features of the equatorial electrojet, *Geophys. J. R. Astron. Soc.*, *56*, 127–138.
- Rastogi, R. (1989), The equatorial electrojet, in *Geomagnetism*, vol. 3, edited by J. Jacobs, pp. 461–525, Academic, San Diego, Calif.
- Rastogi, R. G. (2004), Electromagnetic induction by the equatorial electrojet, *Geophys. J. Int.*, *158*, 16–31.
- Rastogi, R. G., T. Kitamura, and K. Kitamura (2004), Geomagnetic field variations at the equatorial electrojet station in Sri Lanka, Peredinia, *Ann. Geophys.*, *22*, 2729–2739.
- Sabaka, T. J., N. Olsen, and M. Purucker (2004), Extending comprehensive models of the Earth's magnetic field with Ørsted and CHAMP data, *Geophys. J. Int.*, *159*, 521–547, doi:10.1111/j.1365-246X.2004.02421.x.
- Samapth, S., and T. S. G. Sastry (1979), Depth of non-conducting layer in the Indian Ocean region around Thumba, derived from in situ investigations of equatorial electrojet, *J. Geomagn. Geoelectr.*, *31*, 381–389.
- Schmucker, U. (1987), Substitute conductors for electromagnetic response estimates, *Pure Appl. Geophys.*, *125*, 341–367.
- Schmucker, U. (1999), A spherical harmonic analysis of solar daily variations in the years 1964–65—I. Methods, *Geophys. J. Int.*, *136*, 439–454.
- Singh, B. P., N. Nityananda, and A. K. Agarwal (1977), Induced magnetic variation in the Indian Peninsula, *Acta Geodat. Geophys. Montanist. Acad. Sci. Hung. Tomus.*, *12*, 65–72.
- Srivastava, B. J., and S. N. Prasad (1982), Geomagnetic induction anomalies in India in relation to geology, *Geophys. Surv.*, *5*, 193–212.
- Takeda, M., and H. Maeda (1979), Effect of the coastline configuration of south India and Sri Lanka region on the induced field at short period, *J. Geophys.*, *45*, 209–218.
- Thakur, N. K., M. V. Mahashabde, B. R. Arora, R. Singh, B. J. Srivastava, and S. N. Prasad (1981), Anomalies in geomagnetic variations in peninsular India near Palk Strait, *Geophys. Res. Lett.*, *8*, 947–950.
- Van'yan, L. L., E. B. Faynberg, and N. Y. Genis (1975), Deep sounding of the earth by ground-based and satellite measurements of the magnetic field of the equatorial electrojet, *Geomagn. Aeron.*, *15*, 112–116.
- Vassal, J., M. Menvielle, Y. Cohen, M. Dukhan, V. Doumouya, K. Boka, and O. Fambitakoye (1998), A study of transient variations in the Earth's electromagnetic field at equatorial electrojet latitudes in western Africa (Mali and the Ivory Coast), *Ann. Geophys.*, *16*, 677–697.
- Yacob, A. (1977), Internal induction by the equatorial electrojet in India examined with surface and satellite geomagnetic observations, *J. Atmos. Terr. Phys.*, *39*, 601–606.

A. Kuvshinov, Institute of Geophysics, ETH-Zurich, Schafmattsstrasse 30, CH-8093 Zurich, Switzerland. (kuvshinov@erdw.ethz.ch)

C. Manoj, National Geophysical Research Institute, Uppal Road, Hyderabad-500007, India.

N. Olsen, Danish National Space Center, Juliane Maries Vej 30, DK-2100 Copenhagen, Denmark.

T. Sabaka, Planetary Geodynamics Laboratory, NASA GSFC, Code 698 Greenbelt, MD 20771, USA.